Int. J. Heat Mass Transfer. Vol. 32, No. 10, pp. 1967–1978, 1989
Printed in Great Britain

0017–9310/89 $3.00+0.00

Turbulent natural convection of gases in horizontal cylindrical annuli at cryogenic temperatures

ANDREW E. McLEOD† and EUGENE H. BISHOP
Department of Mechanical Engineering, Clemson University, Clemson, SC 29631, U.S.A.

(*Received* 14 *June* 1988 *and in final form* 24 *February* 1989)

Abstract—An experimental study of heat transfer by natural convection of helium between horizontal isothermal concentric cylinders at cryogenic temperatures is performed. Overall heat transfer rates, profiles of the time-averaged temperature, and temperature fluctuations are measured for Rayleigh numbers of 8×10^6–2×10^9 and for expansion numbers of 0.25–1.0. An equation is presented which correlates the heat transfer data in terms of the expansion number and a Rayleigh number based on the inner- and outer-cylinder diameters. The influence of the Rayleigh number and the expansion number on the time-averaged temperature profiles and the temperature fluctuations is reported. The nature and extent of turbulence in the convective flow, as reflected in the fluctuations of temperature, are also documented.

INTRODUCTION

NATURAL convection heat transfer in enclosures is an important class of thermal problems that has application in electronic cooling, high-voltage cable cooling, solar energy collectors, and nuclear reactors. The specific topic of natural convection between isothermal horizontal concentric cylinders has been the subject of much research over the past 25 years, and there have been several correlations presented for the average heat transfer between the cylinders. Both analytical and empirical equations have been proposed that include the effects of the Rayleigh number, the Prandtl number, geometry and recently, the expansion number $\beta\Delta T$.

Several researchers have also measured time-averaged temperature fields and have presented qualitative descriptions of principally the laminar flow field using photographic and optical methods. Until recently, there has been only one study which presented results on temperature fluctuations in the convecting gas, especially as the gas flow becomes turbulent. Bishop [1] acknowledged that temperature–time measurements had been made in his study, but only the time-averaged results were presented. This paper extends the heat transfer study of ref. [1] and the initial temperature fluctuation study of Fersner [2]. A brief review of the pertinent literature will now be presented to place the results presented in this paper in the proper context.

The earliest study of natural convection in cylindrical annuli was carried out by Beckman [3] and extended by Kraussold [4] to include Prandtl number variations. Beckman correlated his average heat transfer results in terms of the equivalent thermal conductivity

$$K_{eq} = K_{eff}/k \tag{1}$$

where k is the thermal conductivity of the convecting fluid and K_{eff} the effective conductivity or the conductivity a stationary fluid would need to have to transfer the same amount of heat as a convecting fluid under the same cylinder temperature difference. The equivalent thermal conductivity is defined as

$$K_{eq} = Q\ln(D_o/D_i)/2\pi L_s\Delta Tk. \tag{2}$$

Liu *et al.* [5] determined the effect of diameter ratio and Prandtl number on the overall heat transfer rate and correlated their results in the functional form

$$K_{eq} = K_{eq}(Pr\,Gr_L)$$

where $Pr\,Gr_L$ represents the Rayleigh number based on annulus width L. Thermocouple probes were used to obtain temperature profiles in the annulus and photographic studies were also used to determine the flow patterns up to $Ra_L = 4\times10^7$, where laminar flow oscillations were observed. Grigull and Hauf [6] provided detailed descriptions of temperature fields and laminar flow structures for air at several diameter ratios through the use of interferometry and smoke.

Lis [7] extended the maximum Rayleigh number to around 10^{10} by using pressurized nitrogen and sulfur hexafluoride in the annulus. He found that Ra_L did not adequately account for diameter ratio effects. Lis used Schlieren observations to give qualitative descriptions of the flow field. He reported irregular oscillations in the thermal plume-like structure above the inner cylinder at $Ra_{D_i} = 5.5\times10^5$ and found the first signs of turbulence in the outer-cylinder flow at $Ra_{D_i} = 1.4\times10^6$. His maximum flow observation Rayleigh number was 7×10^7 at which he reported increased turbulence in the flow adjacent to the outer

† Now at: Tennessee Eastman Company, Engineering Division, Kingsport, TN 37662, U.S.A.

NOMENCLATURE

c_p	specific heat [J kg^{-1} K^{-1}]
D_i	inner-cylinder diameter [m]
D_o	outer-cylinder diameter [m]
g	acceleration due to gravity [m s^{-2}]
Gr_L	Grashof number based on L, $\rho^2 g\beta\Delta T L^3/\mu^2$
k	thermal conductivity [W m^{-1} K^{-1}]
K_{eff}	effective thermal conductivity $Q \ln (D_o/D_i)/2\pi L_s \Delta T$ [W m^{-1} K^{-1}]
K_{eq}	equivalent thermal conductivity, K_{eff}/k
L	annulus width, $(D_o - D_i)/2$ [m]
L_s	length of the test section [m]
M, N	empirical constants
Pr	Prandtl number, $\mu c_p/k$
Q	heat removed by convection [W]
Q_{in}	total power input to the test heater [W]
Q_{loss}	heat lost by end conduction and radiation [W]
R	radial coordinate [m]
R_i	inner-cylinder radius [m]
R_o	outer-cylinder radius [m]
Ra_{D_i}	Rayleigh number based on inner diameter, $g\beta\Delta T D_i^3/\nu\alpha$
Ra_L	Rayleigh number based on L, $g\beta\Delta T L^3/\nu\alpha$
Ra^*	Rayleigh number based on D_o and D_i as defined by Raithby and Hollands [10], $\{[\ln (D_o/D_i)]^4/L^3(D_i^{-3/5} + D_o^{-3/5})^5\} Ra_L$
$\bar{T}$	time-averaged helium temperature [K]
T_i	inner-cylinder surface temperature [K]
T_o	outer-cylinder surface temperature [K]
ΔT	temperature difference, $T_i - T_o$ [K]
T_j	instantaneous helium temperature [K]
T_{ref}	volume-weighted mean helium temperature [K]
Z	dimensionless radial coordinate, $(R - R_i)/(R_o - R_i)$.

Greek symbols

β	volumetric coefficient of thermal expansion [K^{-1}]
$\beta\Delta T$	expansion number
θ	Dimensionless time-averaged helium temperature, $(\bar{T} - T_o)/(T_i - T_o)$
μ	viscosity of the test gas [kg m^{-1} s^{-1}]
ν	kinematic viscosity of the test gas [m^2 s^{-1}]
ρ	density of the test gas [kg m^{-3}]
σ	normalized standard deviation of temperature, $\{\Sigma (T_j - \bar{T})^2/(N-1)\}^{1/2}/(T_i - T_o)$
ϕ	angle measured positive downward from the upward vertical [deg].

Subscripts

D_i	inner-cylinder diameter
eff	effective
eq	equivalent
i	inner-cylinder surface
j	instantaneous value
L	annulus width
o	outer-cylinder surface
ref	reference
s	test section.

Superscripts

*	based on D_o and D_i.

cylinder but no change in the stable laminar inner-cylinder flow. Bishop and Carley [8] presented detailed descriptions and photographs of stable laminar and oscillating laminar flow patterns in the annulus. Bishop *et al.* [9] presented correlating equations for the prediction of the inception of the oscillatory flow in the plume above the inner cylinder and equations for its amplitude, period, and wavelength.

Raithby and Hollands [10] and Kuehn and Goldstein [11–13] presented overall heat transfer equations based on semi-empirical conduction layer models which included appropriate Rayleigh number and diameter ratio effects. Raithby and Hollands' correlation included Prandtl number effects but was restricted to laminar flow conditions. Kuehn and Goldstein [13] utilized optical methods to obtain temperature distributions and local heat transfer coefficients for nitrogen up to $Ra_L = 8 \times 10^7$. They presented detailed qualitative descriptions of the flow conditions based on interferogram interference patterns and reported turbulent flow in the entire plume and top half of the inner cylinder at $Ra_L = 8 \times 10^7$.

The most recent reported experimental study on this subject was conducted on the same basic apparatus used in the experiments described in this paper. Bishop [1] conducted overall heat transfer tests and concluded that the expansion number $\beta\Delta T$ must be considered along with the Rayleigh number in determining the heat transfer, as the non-dimensional form of the governing equations suggest [14]. Bishop proposed the following correlation for a diameter ratio of 3.37:

$$K_{eq} = 0.189 \exp (0.21 \beta\Delta T) Ra_L^{0.25} \quad (3)$$

for $0.2 \leqslant \beta\Delta T \leqslant 0.9$ and $2 \times 10^6 \leqslant Ra_L \leqslant 2 \times 10^9$. He used time-averaged temperature profiles to support his conclusion of a $\beta\Delta T$ effect by analyzing the temperature gradients at the cylinder walls for various $\beta\Delta T$ values at the same magnitude of the Rayleigh number. Fersner [2] reported in his Master's thesis

detailed temperature field information and used a spectral density analysis of instantaneous temperature measurements for a diameter ratio of 3.37 to show predominant oscillation frequencies and, based on this temperature information, proposed the spatial extent of turbulent flow in the annulus. His results were not conclusive, but general trends found in his study were confirmed by the data of this study. Fersner was the first to make direct, high sample rate temperature measurements in this geometry, and his measurement technique was employed in this investigation.

This paper presents the results of a detailed experimental study of high Rayleigh number natural convection of helium between horizontal, isothermal concentric cylinders at cryogenic temperatures with Prandtl number $Pr = 0.688$, diameter ratio $D_o/D_i = 4.85$, and with values of the expansion number $\beta\Delta T$ up to 1.0. The apparatus used in ref. [1] was used in this study with only a change in the diameter of the inner cylinder. The inner cylinder was maintained at temperatures higher than the outer cylinder in all tests. The experimental results are presented in the following manner:

(1) an overall correlation equation of heat transfer in terms of the expansion number and a modified Rayleigh number (originally proposed by Raithby and Hollands [10]) that accounts for the inner- and outer-cylinder diameters;

(2) time-averaged temperature profiles for selected annulus locations;

(3) profiles of the standard deviation of temperature fluctuations at selected locations; and

(4) instantaneous temperature–time traces and spectral density plots at selected locations.

To the author's knowledge, this is the first publication of temperature fluctuation data in cylindrical annuli at high Rayleigh numbers, and the data should be useful to those studying flow transitions and proposing turbulent flow models.

APPARATUS AND PROCEDURES

Figure 1 is a schematic diagram of the experimental setup. The basic test apparatus, as described in ref. [1], consists of a 0.0409 m o.d., heated copper inner test cylinder support concentrically in a 0.203 m i.d., cooled, stainless-steel outer test cylinder. These two cylinders are supported concentrically in a larger diameter stainless-steel cylinder that is well insulated on its outside surface. The annular space between the outer test cylinder and this cylinder is used as a cooling jacket for maintaining the outer test cylinder at a constant temperature. Liquid nitrogen was continually fed to this cooling jacket during the test, and the cooling bath was vented to the atmosphere such that the outer-cylinder temperature was maintained at approximately the saturation point of liquid nitrogen (77.35 K). The stainless-steel outer test cylinder and the cooling-jacket cylinder are both welded to stainless-steel end plates. The end plates were maintained at close to liquid nitrogen temperature by passing liquid nitrogen through heat exchangers that were attached to the plates at both ends of the apparatus. The end plates are also well insulated. The inner test cylinder is secured concentrically in the outer test cylinder by a bolt–flange arrangement at the left end plate with a metal 'O'-ring seal to permit pressurization or evacuation of the annulus gas. The annulus was pressurized by connecting it to a pressurized bottle of helium through a pressure regulator or it was evacuated by a vacuum pump. The liquid nitrogen charging system consists of three 50 l dewars with liquid discharge devices connected in series. The charge line is connected to the end plate and flange heat exchangers and to the cooling jacket.

The inner test cylinder is a 31.8 cm long, 4.19 cm diameter copper section of the inner cylinder. The right end of the cylinder is capped with a hollow nylon cylinder filled with fiberglass insulation, and the left end is attached through a metal 'O'-ring seal to a stainless-steel cylinder, which is welded to the flange and inside of which is placed fiberglass insulation. The temperature of the inner cylinder was controlled by varying the power input to an electrical resistance heater embedded along the axis of the copper cylinder. The temperature of the cylinder was measured at nine locations by copper–constantan thermocouples affixed to the cylinder in three, 0.476 cm diameter holes drilled 120° apart, parallel to the axis of the cylinder. The thermocouples were inserted to three longitudinal depths and epoxied to the copper surface. Alumina was packed in the holes after each thermocouple was in place. The inner-cylinder temperature was taken to be a weighted average of these nine thermocouple readings. All thermocouple wires and electrical leads were contained within the inner cylinder and brought out through the flange support end of the cylinder.

Five temperature probe passages were located along the center plane of the annulus at 30° intervals from the top vertical to the 120° position. Special probe holders were designed that permitted probing while the annulus was under pressure. The probes were specially modified TSI model 1248 hot-wire anemometer probes, which were used in a constant current circuit with the voltage drop across the sensing element being monitored. The probes were traversed radially across the annulus at each of the five angular positions using a 'Unislide' traversing mechanism with a least count of 0.001 cm. The voltage output was measured and stored on a Digital Equipment Corporation MINC 1103 data acquisition computer. The uncertainty in the measurement of the helium temperature is estimated to be ± 0.5°C. A complete description of the apparatus is contained in a Master's thesis by McLeod [14].

Since only heat transfer by natural convection was being sought, it was necessary to determine the radi-

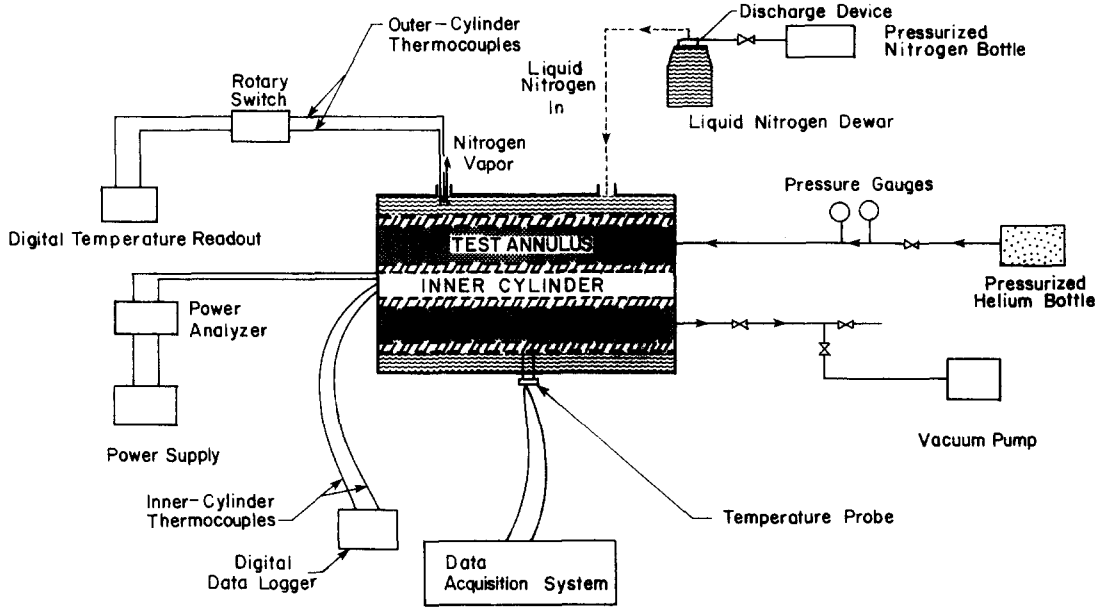

FIG. 1. Schematic of experimental system.

ation transfer and longitudinal conduction loss through the inner cylinder to the end plates. These heat transfer rates were experimentally determined by evacuating the gap between the cylinder to a pressure of about 15 N m^{-2}. At this pressure and at the maximum inner-cylinder temperature used for the convection tests of 200 K, convection and gas conduction between the cylinder surfaces is insignificant. By maintenance of a constant outer-cylinder temperature at approximately 77 K for the calibration, the sum of the radiation and longitudinal conduction losses becomes a function of only the temperature of the inner cylinder and is essentially equal to the total power input to the electrical resistance heater. The power input to the heater was set to a sufficient number of values to permit plotting a calibration curve over a range of inner-cylinder temperatures from about 100 to 222 K with variances of ± 0.2 and ± 4.0 K, respectively. About 10 h were allowed for each calibration point to assure steady-state conditions. A second-order quadratic equation was fitted to the calibration points to yield

$$Q_{\text{loss}} = 0.00025T_i^2 + 0.00309T_i - 1.8111. \quad (4)$$

The uncertainty in Q_{loss} is estimated to be ± 0.17 W.

Thirty-three heat transfer runs were conducted with helium at pressures from 1.5 to 18 atm in the annulus. Since the primary objective of the experiments was to determine the effects of varying the expansion number on the heat transfer, it was necessary to hold this parameter constant at several values while varying the Rayleigh number. This required that the inner-cylinder temperature not change while the Rayleigh number was changed by increasing or decreasing the pressure of the helium in the annulus. The inner-cylinder temperature was kept constant as the pressure was changed by adjusting the power input to the inner-cylinder heater either up or down depending upon whether the pressure was increased or decreased. Eleven different values of the Rayleigh number ranging from 8×10^6 to 2×10^9 were tested at each of three constant expansion numbers of approximately 0.25, 0.5 and 1.0. Normally 2–3 h were allowed for the establishment of a steady state before each recording. Steady-state conditions were assumed after the nine inner-cylinder thermocouples indicated less than a 0.1 K change in temperature over a 15 min period of time. The outer cylinder was maintained at the same temperature as that used for the calibration so that equation (4) could be used to predict the heat loss at a variety of inner-cylinder temperatures. For the heat transfer runs the heat loss varied from about 1.5 to 5.5% of the total power input to the heater.

Temperature traverses were made at Rayleigh number values of approximately 10^7, 10^8 and 10^9 for each of the three expansion numbers. Temperatures were measured at 21 radial locations between the inner- and outer-cylinder surfaces at each of the five angular positions. Spacings of 1 mm were used near both cylinder surfaces while 5 and 10 mm spacings were used for the bulk of the annulus. Each measurement was taken at a frequency of 50 samples per second over a 20.48 s time period for a total of 1024 samples per position.

HEAT TRANSFER

To reduce the heat transfer data and present them in an appropriate dimensionless form, the volume-weighted reference temperature recommended by Bishop [1] was used to evaluate the thermodynamic

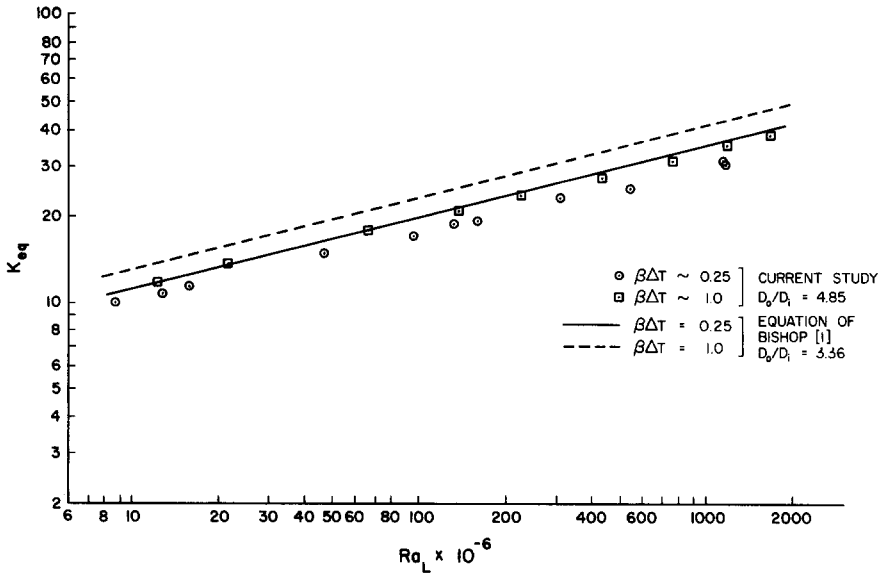

FIG. 2. Heat transfer data at $\beta\Delta T = 0.25$ and 1.0 compared to Bishop's equation.

and transport properties. This temperature is defined as

$$T_{ref} = [(R_{avg}^2 - R_i^2)/(R_o^2 - R_i^2)]T_i + (R_o^2 - R_{avg}^2)/(R_o^2 - R_i^2)]T_o. \quad (5)$$

For the cylinder combination of this study, the reference temperature given by equation (5) reduces to

$$T_{ref} = 0.335T_i + 0.664T_o. \quad (6)$$

By using equation (6) to evaluate the properties, any variation found in the heat transfer rate at a given Rayleigh number for different magnitudes of the expansion number would be due principally to changes in the expansion number.

The heat transfer rates were nondimensionalized by calculating the equivalent thermal conductivity K_{eq} defined by equation (2). Figure 2 is a log–log plot of K_{eq} vs Ra_L for approximately constant expansion numbers $\beta\Delta T$ of 0.25 and 1.0. Bishop's correlation equation, equation (3), is plotted for comparison. For the larger expansion number, an upward shift similar to the prediction of Bishop's equation is evident in the data. The plot also shows the effect of increasing the diameter ratio from 3.37 to 4.85. The log–log plot of the data in Fig. 2 shows that the data points fall along approximately straight lines with slopes similar to that of Bishop's data. This implies a simple power relation for K_{eq} as a function of the Rayleigh number, with an exponent close to that of the exponent on the Rayleigh number in Bishop's correlation, equation (2). Also, semi-log plots of K_{eq} vs $\beta\Delta T$ for fixed values of the Rayleigh number give lines of constant slopes similar to Bishop's results. This implies a simple exponential relation for the expansion number effect on K_{eq}. Thus, the form of the correlating equation, excluding diameter ratio effects, was assumed to be

$$K_{eq} = C[\exp(\beta\Delta T)]Ra_L^M \quad (7)$$

where M and N are constants approximately equal to those of Bishop.

Since only one additional diameter ratio was tested, the combined data of this study and the previous study by Bishop was not sufficient to determine a diameter ratio effect. The literature was searched to find a diameter ratio or geometry relation which had been successful in the past in correlating heat transfer results for a range of diameter ratios. The relation used by Raithby and Hollands [10] was chosen because it had been developed from an analytical model and was successful in correlating experimental data from a number of investigators and over a significant range of values of the diameter ratio. Raithby and Hollands incorporated the diameter ratio effect in a modified Rayleigh number defined as

$$Ra^* = \{[\ln(D_o/D_i)]^4/L^3(D_i^{-3/5} + D_o^{-3/5})^5\}\, Ra_L. \quad (8)$$

The Rayleigh number in equation (7) was changed to Ra^*, and a least squares technique was used to determine the constants C, M and N for the combined data of this study and Bishop's study. The following equation was determined:

$$K_{eq} = 0.306 \exp(0.174\beta\Delta T)(Ra^*)^{0.245} \quad (9)$$

which is valid for $0.2 \leqslant \beta\Delta T \leqslant 1.0$, $6 \times 10^6 \leqslant Ra_L \leqslant 2 \times 10^9$, $Pr = 0.688$ and $3.0 \leqslant D_o/D_i \leqslant 5.0$. All properties are evaluated at the volume-weighted mean reference temperature given by equation (6). Equation (9) is shown plotted with all of the data of Bishop and this study in Fig. 3. The correlation gives deviations from the experimental data ranging from -10.4 to 13.8% with a standard deviation of 6.5% where deviation is defined by

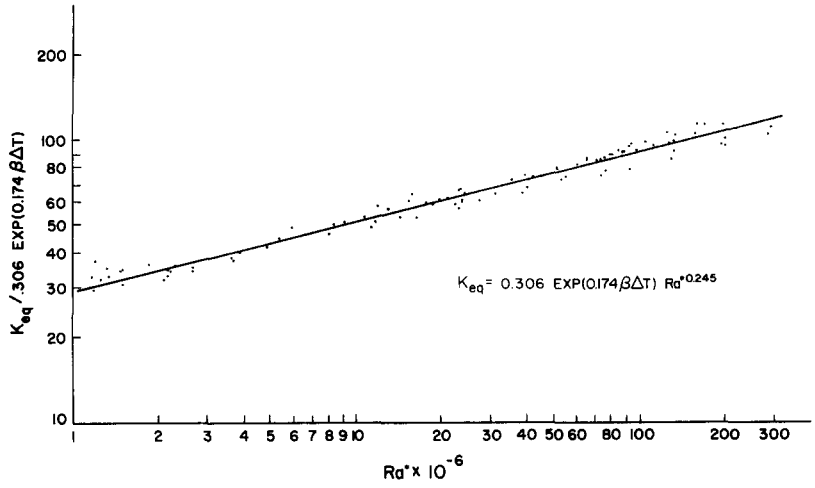

FIG. 3. Overall correlation of the heat transfer data of Bishop and the present study.

$$\%\text{Deviation} = [(K_{eq})_{\text{equation}} - (K_{eq})_{\text{data}}]/(K_{eq})_{\text{data}} \times 100.$$

The uncertainties in the experimental measurements and in the values of the transport properties combine to give maximum possible errors in the Rayleigh number, equivalent conductivity, and expansion number of ± 7.5, ± 6.2 and $\pm 4.6\%$, respectively.

TEMPERATURE DISTRIBUTIONS

The instantaneous temperatures measured in the annulus gas were time averaged at all measurement locations to permit plotting profiles of the average temperature in the convective flow. These plots of average temperature were evaluated to determine qualitative information about local heat transfer rates, flow patterns and turbulence levels.

Figure 4 is a plot of the non-dimensional, time-averaged temperature θ vs non-dimensional, radial position Z for five angular positions ϕ, $Ra_L = 1.22 \times 10^7$ and $\beta\Delta T = 1.0$. These profiles agree well with the results of Bishop [1] and Fersner [2] who were the first investigators to make direct temperature measurements above $Ra_L = 10^6$. There is evidence of a large, almost isothermal layer of fluid in the central portion of the annulus below $\phi = 30°$, enclosed by thin thermal boundary layers adjacent to each cylinder surface. The temperature of this central core region is much closer to the outer-cylinder temperature than the inner-cylinder temperature, a fact which supports the use of a volume-weighted reference temperature as recommended by Bishop. Temperature inversions exist in the central portion of the annulus at $\phi = 30°$ and $60°$ such that fluid near the cold surface is warmer than fluid closer to the hot surface. Similar inversions in the temperature have been observed by other investigators and are attributed to the effect of the strong recirculating flow.

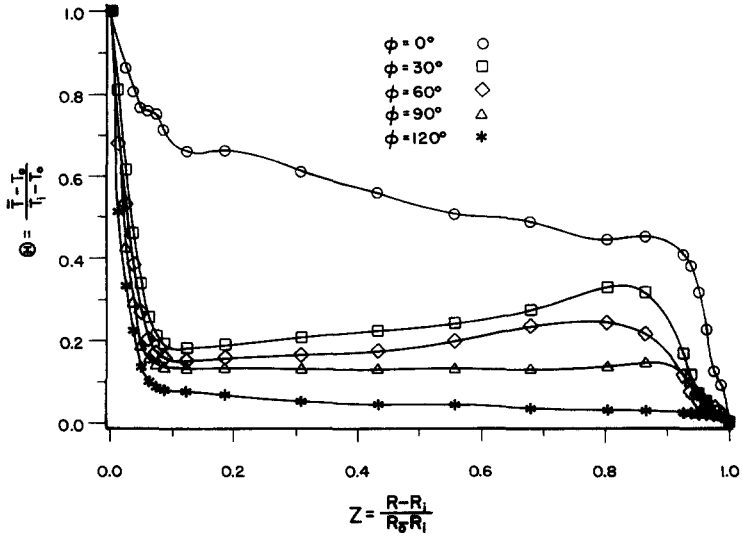

FIG. 4. Dimensionless time-averaged temperature profiles for $Ra_L = 1.22 \times 10^7$, $\beta\Delta T = 1.0$.

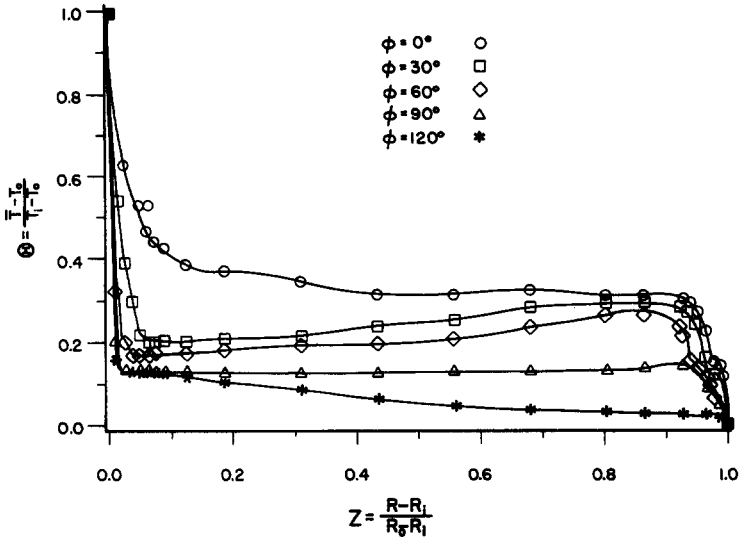

FIG. 5. Dimensionless time-averaged temperature profiles for $Ra_L = 1.18 \times 10^9$, $\beta\Delta T = 0.998$.

A qualitative comparison of the local surface heat transfer rates on the inner- and outer-cylinder surfaces can be made from the temperature profiles of Fig. 4 by comparing the relative magnitude of the temperature difference across the thermal boundary layer for different values of ϕ. On the inner cylinder, the heat transfer rate is a maximum at $\phi = 120°$ and decreases to a minimum at $\phi = 0°$. This is reversed on the outer cylinder with a maximum at the top of the annulus and a very low heat transfer rate at $\phi = 120°$ where the temperature drop across the boundary layer is very small. These qualitative conclusions agree well with the results of earlier research at lower Rayleigh numbers.

Profiles of the average temperature for $Ra_L = 1.18 \times 10^9$ and $\beta\Delta T = 1.0$ are shown in Fig. 5. Comparing these profiles with those of Fig. 4, the effects of increasing the Rayleigh number for a fixed value of the expansion number can be observed. The most obvious effect is the general lowering of the temperatures at $\phi = 0°$ to temperatures near those at $\phi = 30°$. This reduction in temperatures is the result of increased turbulence in the upper region of the annulus which causes increased fluid mixing and thus a more uniform temperature. More will be said about this later in the paper. Little change is observed in the relative positions of the 30°, 60°, 90°, and 120° profiles except near both cylinder surfaces where the thermal boundary layer becomes significantly thinner and the temperature gradients steeper. These thinner boundary layers give rise to higher local heat transfer rates which are consistent with the generally recognized effect of increasing values of the Rayleigh number on the overall heat transfer rate. Although not shown in this paper, these same effects were found for expansion numbers of 0.25 and 0.5.

The effect of varying the expansion number on the time-averaged temperature profiles for a fixed magnitude of the Rayleigh number is shown in Fig. 6 for $Ra_L = 10^7$, $\phi = 30°$, and for expansion number extremes of 0.25 and 1.0. As the expansion number is increased from 0.25 to 1.0, there is a general reduction in the temperature in the central annulus region but there is no apparent change in the general form of the profile or in the thickness of the thermal boundary layers at the cylinder surfaces. This same effect was observed at $Ra_L = 10^8$ and 10^9. This decrease in the temperature with increasing expansion number is the result of turbulent mixing along the cold outer cylinder. Changes in the flow structure near the outer-

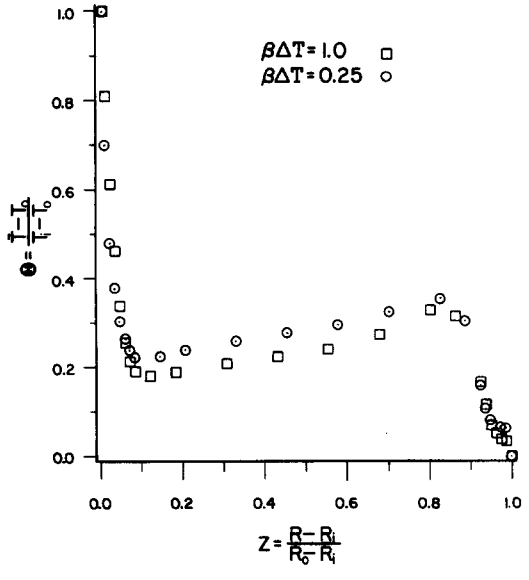

FIG. 6. Dimensionless time-averaged temperature profiles for $\phi = 30°$, $Ra_L = 1 \times 10^7$, $\beta\Delta T = 0.25$ and 1.0.

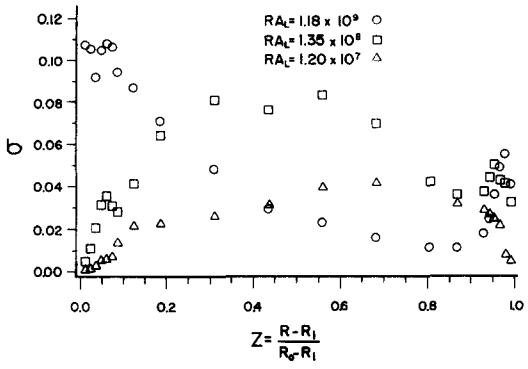

FIG. 7. Dimensionless standard deviation of temperature profiles at $\phi = 0°$, $Ra_L = 1.18 \times 10^9$, 1.35×10^8, 1.20×10^7 and $\beta\Delta T = 1.0$.

cylinder surface for a fixed Rayleigh number occur as the magnitude of the expansion number is increased. This will be discussed in detail in the next section.

TEMPERATURE FLUCTUATIONS

The temperature fluctuation measurements were statistically analyzed to determine the flow structure of the convecting helium gas. An important assumption made in this analysis was that the temperature fluctuations were spectrally analogous to the velocity fluctuations. Although no study has been made that compares temperature and velocity fluctuations for this geometry, studies in other geometries have shown that there is a close coupling of the two parameters for natural convection in general [15–18]. Based on these past results, the qualitative conclusions of this paper concerning the flow structure are considered to be valid.

Plots of standard deviation σ vs non-dimensional radial position Z describe the spatial distribution of the magnitudes of the temperature fluctuations and help to determine the important locations in the flow that need further investigation. Figures 7 and 8 are standard deviation profiles for the 0° and 30° angular positions, respectively, for $\beta\Delta T = 1.0$ and for three

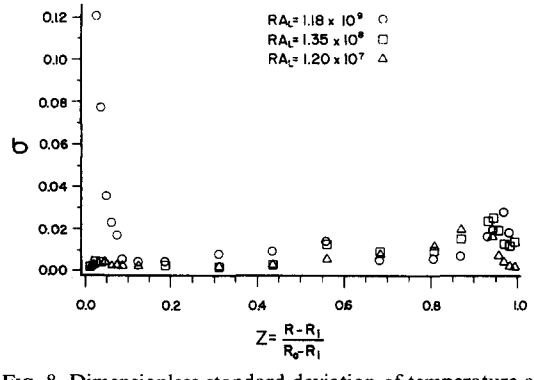

FIG. 8. Dimensionless standard deviation of temperature at $\phi = 30°$, $Ra_L = 1.18 \times 10^9$, 1.35×10^8, 1.20×10^7 and $\beta\Delta T = 1.0$.

Rayleigh numbers. The profile for $Ra_L = 1.2 \times 10^7$ in Fig. 7 shows the effect of the large amplitude, low frequency 'waves' in the plume-like flow rising from the inner cylinder. As will be shown later, the flow in this large scale motion is not turbulent. The flow near both surfaces is very stable as shown by the low values. When the Rayleigh number is increased to 1.35×10^8, the maximum value of σ increases because the amplitude of the plume wave increases. When the Rayleigh number is increased to 1.18×10^9, the curve collapses which indicates a significant change in the flow structure.

Figure 8 is the standard deviation plot for the 30° angular position for the same Rayleigh numbers as in Fig. 7. There is a large proportion of the annulus that sees only small fluctuations in the temperature which indicates a large stagnant region. The σ magnitudes adjacent to both cylinder surfaces show the effects of the relatively high speed boundary-layer like flow, and the outer-cylinder profiles tend to come together as the Rayleigh number is increased, but the maximum values are roughly the same. As with the 0° profile, a dramatic change occurs at $Ra_L = 1.18 \times 10^9$. The magnitude of the fluctuations increases significantly adjacent to the inner-cylinder surface. The σ profiles for the 60°, 90°, and 120° positions are very similar to Fig. 8 except for a reduction in the magnitudes of the peak values as ϕ increases. At the 120° position, there are no significant fluctuations on either cylinder surface. Although not presented here, σ plots for expansion numbers of 0.5 and 1.0 were also made with results very similar to those just described.

Temperature–time and spectral plots were made where peaks in the standard deviation plots occurred near the cylinder surfaces and in the plume region. These plots helped to described the structure of the temperature fluctuations. When low frequency , large spikes were found in the power spectral density plots, laminar oscillating or transition flow was assumed. When these low frequency harmonics spread to form a broad band of frequencies, turbulent flow was assumed. In the following discussion, a few key examples of the many measurement locations and parameter values examined will be presented.

As discussed in the temperature distribution section and in the standard deviation results, the plume flow at the 0° position undergoes a drastic change at $Ra_L = 10^9$. This flow change was examined by use of the instantaneous temperature results, and typical examples are shown in Figs. 9 and 10. These figures show the temperature–time traces and spectral plots for the 0° position at approximately half way between the cylinders. In Fig. 9 for $Ra_L = 1.27 \times 10^7$ and $\beta\Delta T = 0.26$, the laminar oscillations of the plume are apparent since the spectral plot shows only strong low frequency fluctuations. This same type of flow was observed for $Ra_L = 10^8$. In both cases, the frequencies closely match the predictions in ref. [9]. As shown in Fig. 10 for $Ra_L = 1.15 \times 10^9$ and $\beta\Delta T = 0.24$, the flow structure changes completely with the low frequency,

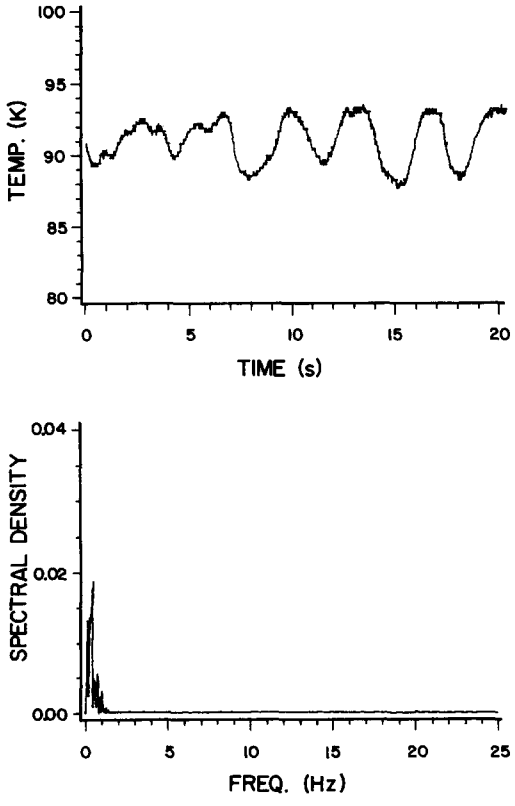

FIG. 9. Temperature–time trace and spectral density plot for $Ra_L = 1.27 \times 10^7$, $\beta\Delta T = 0.26$, $\phi = 0°$, and $Z = 0.335$.

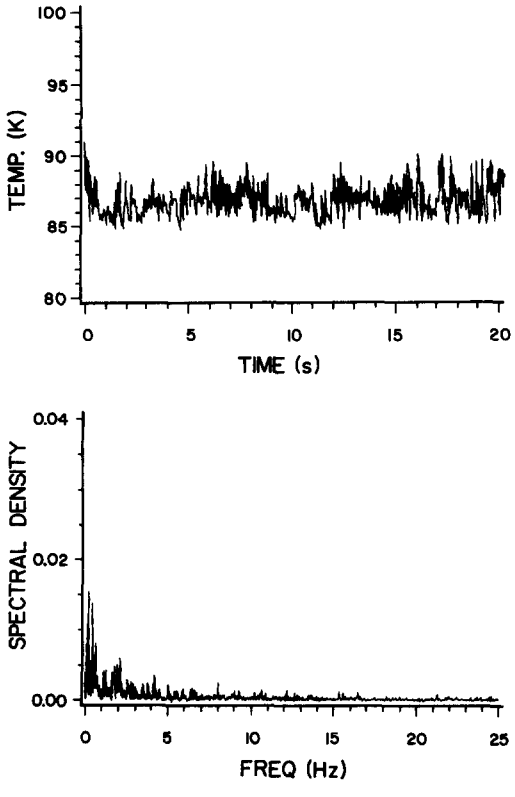

FIG. 10. Temperature–time trace and spectral density plot for $Ra_L = 1.15 \times 10^9$, $\beta\Delta T = 0.25$, $\phi = 0°$, and $Z = 0.310$.

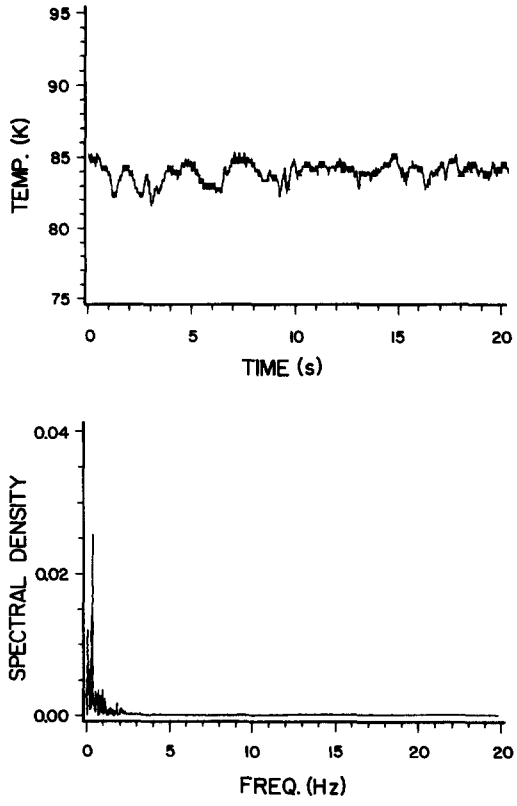

FIG. 11. Temperature–time trace and spectral density plot for $Ra_L = 1.27 \times 10^7$, $\beta\Delta T = 0.26$, $\phi = 30°$, and $Z = 0.893$.

large-scale fluctuations being replaced by multiple, higher frequency fluctuations. The spectral plot displays a broad frequency band characteristic of turbulence. The increased turbulent mixing of the plume fluid with cooler fluid adjacent to the outer cylinder explains the general lowering of the time-averaged temperature profiles at $\phi = 0°$ as the Rayleigh number is increased from approximately 10^7 to 10^9 as shown in Figs. 4 and 5. Also, the collapse of the standard deviation plot at 0° as Ra_L is increased from 10^7 to 10^9 is believed to be the result of the turbulent flow attenuating the large-scale motion required to give such large values of σ.

Examination of the temperature–time traces and spectral plots in the boundary layer adjacent to the inner-cylinder surface indicated little or no fluctuations at $Ra_L = 10^7$ and 10^8. At $Ra_L = 10^9$, a flow transition was found to occur along the inner cylinder. Very large low frequency fluctuations in temperature began at 120° and grew in magnitude until the flow became turbulent at 0°. This transition explains the relatively large σ values adjacent to the inner-cylinder surface for $Ra_L = 10^9$ (refer to Figs. 7 and 8).

The effect of increasing the expansion number for a fixed value of Rayleigh number was an important part of this study, and Figs. 11 and 12 give good examples of this effect on the flow characteristics. Both figures are for $\phi = 30°$ and for a radial location near the outer-cylinder surface. Temperature–time

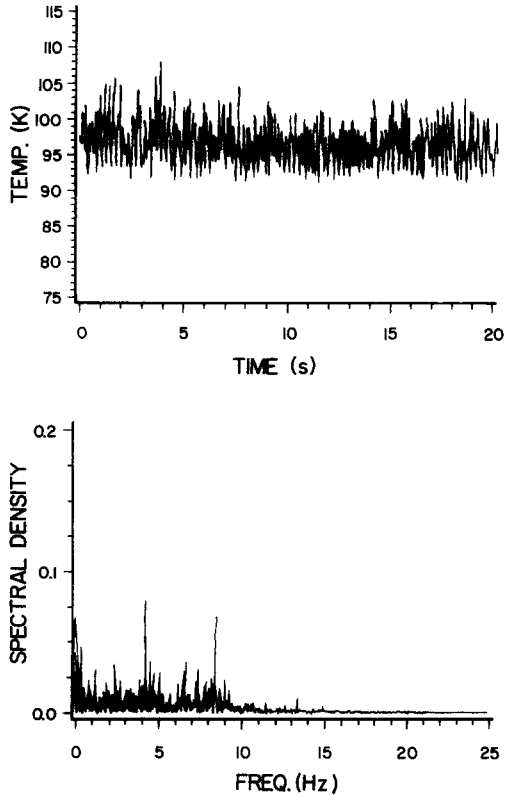

FIG. 12. Temperature–time trace and spectral density plot for $Ra_L = 1.20 \times 10^7$, $\beta\Delta T = 1.00$, $\phi = 30°$, and $Z = 0.930$.

traces and spectral plots are shown in Fig. 11 for $Ra_L = 1.27 \times 10^7$ and $\beta\Delta T = 0.26$ and show fluctuations which are laminar in nature and which have characteristic frequencies similar to the plume's oscillations. Figure 12 is for the same Rayleigh number, but for $\beta\Delta T = 1.0$, at which much higher frequency fluctuations are present and the spectrum indicates a much broader band of frequencies than for $\beta\Delta T = 0.26$. Therefore, it is concluded that an increase in the expansion number from 0.25 to 1.0 results in a change to a more turbulent flow structure. This same effect of more developed turbulent structure in the flow for increasing $\beta\Delta T$ was found at several locations in the annulus. Since higher heat transfer coefficients are associated with turbulence, these results support the conclusion of a $\beta\Delta T$ effect on the heat transfer coefficient.

A summary of the postulated flow structures as determined by the temperature–time traces and spectral plots is presented in the sketches of Figs. 14–17. Figure 13 is a key to the symbols used in describing the flow structures. In Figs. 14 and 15, the flow conditions for $Ra_L = 10^7$ are sketched for $\beta\Delta T = 0.25$ and 1.0, respectively. The effect of increasing the expansion number on the spacial extent of the turbulence is depicted in these sketches. Figures 16 and 17 show the dramatic changes in the flow structure as the Rayleigh number is increased to 10^9. Once again, the increased spatial extent of the turbulence for the

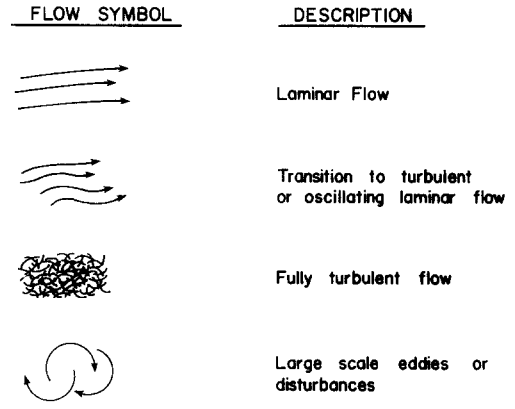

FIG. 13. Key to the flow symbols used in the sketches of Figs. 14–17.

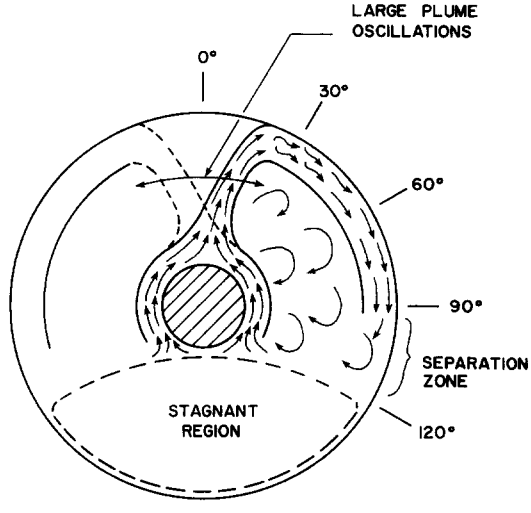

FIG. 14. Postulated flow structure in the annulus for $Ra_L \cong 10^7$ and $\beta\Delta T \cong 0.25$.

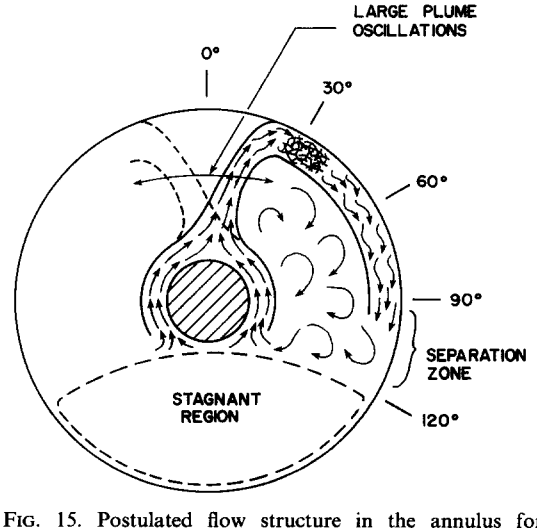

FIG. 15. Postulated flow structure in the annulus for $Ra_L \cong 10^7$ and $\beta\Delta T \cong 1.0$.

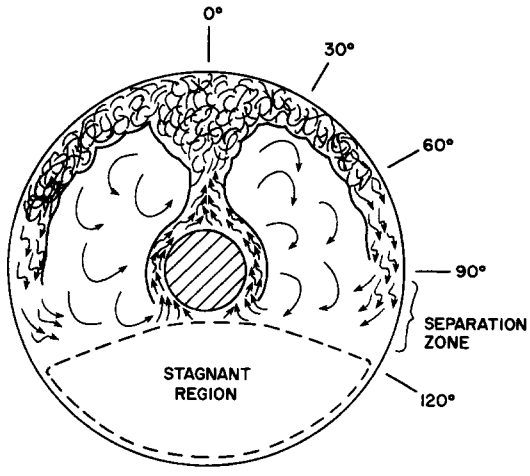

FIG. 16. Postulated flow structure in the annulus for $Ra_L \cong 10^9$ and $\beta\Delta T \cong 0.25$.

higher value of the expansion number is evident in the comparison of these two sketches. Although the temperature fluctuation results for the test at $\beta\Delta T = 0.5$ and $Ra_L = 10^8$ are not presented here, they were examined and were found to follow the same trends.

CONCLUSIONS

An empirical equation has been presented which correlates the heat transfer data and accounts for the effect of the Rayleigh number, the expansion number and the diameter ratio over the ranges $8 \times 10^6 \leqslant Ra_L \leqslant 2 \times 10^9$, $0.25 \leqslant \beta\Delta T \leqslant 1.0$, and $D_o/D_i = 3.37$ and 4.85. The heat transfer results indicated that the expansion number, independent of the Rayleigh number, must be accounted for in the prediction of the heat transfer rates, as was first proposed in ref. [1]. The modified Rayleigh number proposed by Raithby and Hollands [10] was found to adequately account for diameter ratio changes.

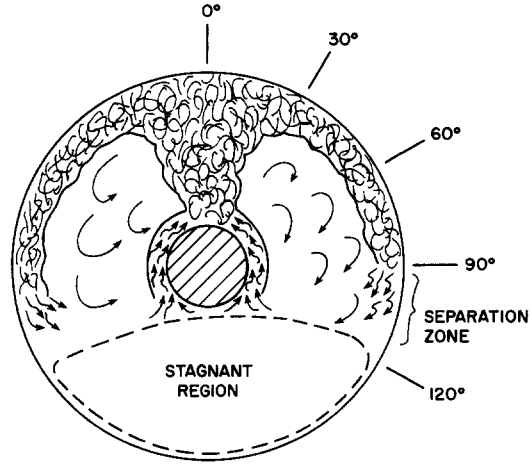

FIG. 17. Postulated flow structure in the annulus for $Ra_L \cong 10^9$ and $\beta\Delta T \cong 1.0$.

Time-averaged temperature profiles of the annulus gas were qualitatively shown to support the effect of varying the magnitude of the Rayleigh number and the expansion number on the overall heat transfer rate. These profiles also agreed well with the results of other investigators where comparisons could be made.

Temperature fluctuation data in the form of standard deviation profiles, temperature–time traces, and spectral plots were used to make conclusions about the flow structure and the spatial extent of turbulence in the annulus as the Rayleigh number and expansion number were varied. A new flow structure in the upper region of the annulus was found. It was also discovered that by increasing the expansion number for a constant Rayleigh number more developed turbulence existed at given annulus locations. This finding supports the conclusion of an independent expansion number effect on the overall heat transfer rate.

Acknowledgment—The authors wish to acknowledge that this material is based upon work supported by the National Science Foundation under Grant No. CBT-8403467 and that the work was carried out in the Thermal/Fluids Science Research Laboratory, which was made possible by a grant from the National Science Foundation under the EPSCOR Program.

REFERENCES

1. E. H. Bishop, Heat transfer by natural convection of helium between horizontal isothermal concentric cylinders at cryogenic temperature, *J. Heat Transfer* **110,** 109–115 (1988).
2. J. W. Fersner, Natural convection between horizontal isothermal concentric cylinders: the temperature field, M.S. thesis, Clemson University, Clemson, South Carolina (1986).
3. W. Beckman, Die Warmeubertragung in zylindrischen Gasschichten bei naturlicher Konvektion, *Forsch. Geb. IngWes.* **2,** 165–178 (1931).
4. H. Kraussold, Warmeabgade von zylindrischen Flussigkeitsschichten bei naturlicher Konvektion, *Forsch. Geb. IngWes.* **5,** 186–191 (1934).
5. C. Y. Liu, W. K. Mueller and F. Landis, Natural convection heat transfer in long cylindrical annuli, *Int. Dev. Heat Transfer, ASME* **4,** 976–984 (1961).
6. U. Grigull and W. Hauf, Natural convection in horizontal cylindrical annuli, *Proc. Third Int. Heat Transfer Conf.*, Vol. 2, pp. 182–195 (1966).
7. J. Lis, Experimental investigation of natural convection heat transfer in simple and obstructed horizontal annuli, *Proc. Third Int. Heat Transfer Conf.*, Vol. 2, pp. 196–204 (1966).
8. E. H. Bishop and C. T. Carley, Photographic studies of natural convection between concentric cylinders, *Proc. 1966 Heat Transfer Fluid Mechanics Institute*, pp. 63–78 (1966).
9. E. H. Bishop, C. T. Carley and R. E. Powe, Natural convection oscillatory flow in cylindrical annuli, *Int. J. Heat Mass Transfer* **11,** 1741–1752 (1968).
10. G. D. Raithby and K. G. T. Hollands, A general method of obtaining approximate solutions to laminar and turbulent free convection problems, *Adv. Heat Transfer* **11,** 265–315 (1975).
11. T. H. Kuehn and R. J. Goldstein, An experimental and theoretical study of natural convection in the annulus

between horizontal concentric cylinders, *J. Fluid Mech.* **74,** 695–720 (1976).
12. T. H. Kuehn and R. J. Goldstein, Correlating equations for natural convection heat transfer between horizontal circular cylinders, *Int. J. Heat Mass Transfer* **19,** 1127–1134 (1976).
13. T. H. Kuehn and R. J. Goldstein, An experimental study of natural convection heat transfer in concentric and eccentric horizontal cylindrical annuli, *J. Heat Transfer* **100,** 635–640 (1978).
14. A. E. McLeod, Heat transfer by natural convection of helium between horizontal isothermal concentric cylinders at cryogenic temperatures, M.S. thesis, Clemson University, Clemson, South Carolina (1987).
15. R. Cheesewright and K. S. Doan, Space–time correlation measurements in a turbulent natural convection boundary layer, *Int. J. Heat Mass Transfer* **21,** 911–921 (1978).
16. R. R. Smith, Characteristics of turbulence in free convection flow past a vertical plate, Ph.D. thesis, University of London, London (1973).
17. K. S. Doan, Contribution a l'étude de la zone de transition et de la zone de turbulence établie dans un écoulement de convection naturelle sur une plaque plane verticale isotherme, These de Doctorat d'Etates Sciences, Universite de Poitiers (1977).
18. R. L. Manajan and B. Gebhart, An experimental determination of transition limits in a vertical natural convection flow adjacent to a surface, *J. Fluid Mech.* **91,** 131–154 (1979).

CONVECTION NATURELLE TURBULENTE DE GAZ DANS UN ESPACE ANNULAIRE HORIZONTAL, AUX TEMPERATURES CRYOGENIQUES

Résumé—On décrit une étude expérimentale de transfert thermique par convection naturelle de l'hélium entre deux cylindres horizontaux concentriques, pour des températures cryogéniques. On mesure les flux thermiques globaux, les profils de température moyenne dans le temps et les fluctuations de température, pour des nombres de Rayleigh entre 8×10^6 et 2×10^9 et pour des nombres d'expansion de 0,25 à 1,0. Une équation présentée regroupe les données de transfert de chaleur en fonction du nombre d'expansion et du nombre de Rayleigh basé sur les diamètres des cylindres.

TURBULENTE NATÜRLICHE KONVEKTION VON GASEN IN EINEM GASGEFÜLLTEN HORIZONTALEN RINGSPALT BEI CRYOGENEN TEMPERATUREN

Zusammenfassung—Es wird über eine experimentelle Untersuchung des Wärmeübergangs durch natürliche Konvektion von Helium zwischen horizontalen isothermen konzentrischen Zylindern im Bereich cryogener Temperaturen berichtet. Der Gesamtwärmedurchgang, die zeitlich gemittelten Temperaturprofile und die Temperaturschwankungen werden für Rayleigh-Zahlen von 8×10^6 bis 2×10^9 und für Expansions-Zahlen von 0,25 bis 1,0 gemessen. Es wird eine Korrelationsgleichung vorgestellt für den Einfluß der Expansions-Zahl und der Rayleigh-Zahl (abhängig von Innen- und Außendurchmesser des Ringspalts) auf den Wärmedurchgang. Der Einfluß der Rayleigh- und der Expansions-Zahl auf die zeitlich gemittelten Temperaturprofile und die Temperaturschwankungen wird beschrieben. Art und Umfang der Turbulenz der konvektiven Strömung, die sich in den Temperaturschwankungen widerspiegeln, werden dokumentiert.

ТУРБУЛЕНТНАЯ ЕСТЕСТВЕННАЯ КОНВЕКЦИЯ ГАЗОВ В ГОРИЗОНТАЛЬНЫХ ЦИЛИНДРИЧЕСКИХ КОЛЬЦЕВЫХ ЗАЗОРАХ ПРИ КРИОГЕННЫХ ТЕМПЕРАТУРАХ

Аннотация—Экспериментально исследуется естественноконвективный теплоперенос гелия между горизоитальными изотермическими концентрическими цилиндрами при криогенных температурах. Измерены коэффициенты теплопередачи, профили средней по времени температуры и флуктуации температуры в диапазоне значений числа Рэлея 8×10^6–2×10^9 и для геометрического коэффициента от 0,25 до 1,0. Представлено уравнение, описывающее теплоперенос с помощью геометрического коэффициента и числа Рэлея, построенного на разности диаметров внутреннего и внешнего цилиндров. Показано влияние числа Рэлея и геометрического коэффициента на профили средней по времени температуры и флуктуации температуры. Подтверждается также, что флуктуации температуры связаны с характером и степенью турбулентности конвективного потока.